*Chem. Chem. Technol., 2018, Vol. 12, No. 3, pp. 372–378*

Chemical Technology

# LEAD ADSORPTION BY NANO-HYDROXYAPATITE GRANULES IN A FIXED-BED COLUMN

***Mohamad Reza Khademolhosseini[1], Iman Mobasherpour[2, *], Davoud Ghahremani[1]***

https://doi.org/10.23939/chcht12.03.372

**Abstract.** The sorption of $Pb^{2+}$ ions was conducted in a fixed-bed column by using nano-hydroxyapatite granules. The breakthrough and exhaustion time decreased with increasing flow rate, decreasing bed depth and increasing influent lead concentration. The proposed mechanism is a partial dissolution of calcium followed by the precipitation of an apatite by the ion-exchange mechanism with the formula $Ca_{10-x}Pb_x(PO_4)_6(OH)_2$ and $Pb_{10}(PO_4)_6(OH)_2$.

**Keywords**: nano-hydroxyapatite granules, $Pb^{2+}$, adsorption, removal, fixed-bed.

## 1. Introduction

Water pollution is the contamination of water bodies such as lakes, rivers, oceans, and ground water caused by human activities, which can be harmful to organisms and plants. Water pollution by toxic heavy metals through the discharge of industrial waste is a worldwide environmental problem. The presence of heavy metals in streams, lakes, and groundwater reservoirs has been responsible for several health problems with plants, animals, and human beings [1]. Heavy metal contamination exists in an aqueous waste stream from many industries such as metal plating, mining, tanneries, painting, car radiator manufacturing, as well as agricultural sources where fertilizers and fungicidal spray are intensively used [2-4].

Among various heavy metals, $Pb^{2+}$ is found to be the most toxic and has many applications in industries. According to bureau of Iran standard (ISIRI 1053) for drinking water specification, a maximum permissible limit of 0.01 $mgl^{-1}$ for $Pb^{2+}$ is desirable [5] and maximum limit of 25 $\mu gl^{-1}$ per kg body weight for all age groups was established by WHO [6]. Beyond this permissible limit, $Pb^{2+}$ can cause serious health effect such as kidney failure, neurological damages, hypertension [7].

A variety of methods for the remediation of heavy metals from liquid media such as water, groundwater, and industrial wastewaters is known. Remediation techniques for the removal of heavy metals in contaminated groundwater and wastewater include precipitation of dissolved metals; ion exchange, flocculation, and membrane filter processes such as micro- and ultra filtration and reverse osmosis. These methods are expensive and often involve the use of chemicals and generate large amounts of sludge [8].

Among various water-treatment techniques described, adsorption is generally preferred for the removal of heavy metal ions due to its high efficiency, easy handling, availability of different adsorbents and cost effectiveness [9-11].

Hydroxyapatite (HAp) is an ideal material for a long-term containment of contaminants because of its high sorption capacity for actinides and heavy metals, low water solubility, high stability under reducing and oxidizing conditions, availability, and low cost [12]. HAp has been utilized in the stabilization of a wide variety of metals (*e.g.*, Cr, Co, Cu, Cd, Zn, Ni, Pu, Pb, As, Sb, U, Bi and V) by many investigators [13-21]. They have reported the sorption is taking place through the ionic exchange reaction, surface complexation with phosphate, calcium and hydroxyl groups and/or co-precipitation of new partially soluble phases.

However, to the best of our knowledge, there has been little research on the use of hydroxyapatite, and studies focused on the $Pb^{2+}$ adsorption capacity in batch experiments. Moreover, in practical industrial water treatment processes, adsorption in fixed-bed columns is preferable, and the experimental data obtained from the laboratory scale fixed-bed columns are helpful for industrial application [22, 23].

The aim of this study is to determine the nano hydroxyapatite granules ability in removing $Pb^{2+}$ ions by varying bed height, flow rate and initial concentration. The column adsorption models applied in this research were the bed depth/service time (BDST), and Thomas models.

[1] Department of Engineering, Maybod Branch, Islamic Azad University, Maybod, Iran
[2] Ceramics Department, Materials and Energy Research Center, P.O. Box 31787-316, Karaj, Iran
[*] *Iman.Mobasherpour@gmail.com*

## 2. Experimental

### 2.1. Preparation of Adsorbent

Nano hydroxyapatite compounds were prepared by a solution-precipitation method using $Ca(NO_3)_2{\cdot}4H_2O$ (Analar No. 10305) and $(NH_4)_2HPO_4$ (Merck No. 1205) as starting materials and ammonia solution as agents for pH adjustment. Its detailed synthesis procedure is reported elsewhere [24]. The resulting powder was dried at 373 K.

### 2.2. Granulation of Nano Hydroxyapatite Powders

Nano hydroxyapatite powder could not be fed directly in the fixed-bed column system because of clogging water column. In order to overcome this problem, the nano powders had to be granulated into micron-sized using the spray drying method. A specific amount of hydro soluble polyvinyl alcohol (PVA) (Junsel Chemical Co. Ltd., Japan) as the binder was first added to distilled water and stirred for 20 min at 313 K until PVA was completely soluble. Then nano hydroxyapatite powder was gradually added and the suspension was stirred again for additional 15 min and slurry was dispersed. After spray drying, the granulate powder passing through a sieve 50 and 70 US mesh was selected for the fixed-bed column system.

### 2.3. Column Adsorption Experiments

Continuous flow adsorption experiments were conducted in glass columns of 1.0 cm inside diameter. At the top of the column, the influent lead solution (200, 400 and 500 mg Pb/l) was pumped through the nano hydroxyapatite granule packed column (10, 15 and 20 mm), at flow rates of 5, 10 and 15 ml/min, using a peristaltic pump. Samples were collected from the exit of the column at regular time intervals and analyzed for lead residual concentration (GBC 932 Plus atomic absorption spectrophotometer).

### 2.4. Characterization

Transmission electron microscopy (TEM) was used to characterize the particles of HAp before and after adsorption. For this purpose, particles were deposited onto Cu grids, which support a "holey" carbon film. The particles were deposited onto the support grids by deposition from a dilute suspension in acetone or ethanol. The crystalline shapes and sizes were characterized by a diffraction (amplitude) contrast and for crystalline materials, by high resolution (phase contrast) imaging. The crystal phase was identified by powder X-ray diffraction (XRD) using Siemens (30 kV and 25 mA) X-ray diffractometer with Cu Kα radiation (λ = 1.5404 Å) and XPERT software. The morphology of the selected resulting powder after granulation was examined by a Cambridge scanning electron microscope (SEM) operating at 25 kV.

## 3. Results and Discussion

### 3.1. Characteristics of Adsorbent

TEM micrograph of the HAp powders after drying at 373 K is shown in Fig. 1a. The microstructure of the HAp crystalline after drying was almost of needle shape, with a size in the range of 20–30 nm. The crystal structure analysis of HAp particles was performed, using X-ray diffraction, and the obtained diffractograms are represented in Fig. 1b. The reflection patterns matched the ICDD standards (JCPDS) for HAp phase. The patterns only showed the peaks characteristic of HAp with no obvious evidences in the presence of other phases. The broad peaks around (2 1 1) and (0 0 2) planes indicated that the crystallites were very tiny in nature with much atomic oscillations. Fig. 2a shows morphology of nano hydroxyapatite powders after spray drying process. As can be observed, the HAp granulated particles exhibited a semi-spherical shape with sizes about 300 μm. Fig. 2b shows a high magnification view of the granulated particle top surface.

### 3.2. Column Adsorption Experiments

#### 3.2.1. Effect of flow rate

The adsorption columns were operated at different flow rates (5, 10 and 15 ml/min) until no further lead removal was observed. The breakthrough curve for a column was determined by plotting the ratio of $C_e/C_0$ ($C_e$ and $C_0$ are the lead concentrations of effluent and influent, respectively) against time, as shown in Fig. 3. The column performed well at the lowest flow rate (5 ml/min). Earlier exhaustion times were achieved, when the flow rate was increased from 5 to 15 ml/min. The column exhaustion time ($C_e/C_0$ = 0.95) was reduced from 47 to 22 min, with an increase in flow rate from 5 to 15 ml/min. This was due to a decrease in the residence time, which restricted the contact of lead solution to the nano hydroxyapatite granules. At higher flow rates the lead ions did not have enough time to diffuse into the pores of the hydroxyapatite granules and they exited the column before equilibrium occurred. Similar results have been found for As(III) removal in a fixed-bed system using a modified calcined bauxite and for color removal in a fixed-bed column system using a surfactant-modified zeolite [25, 26].

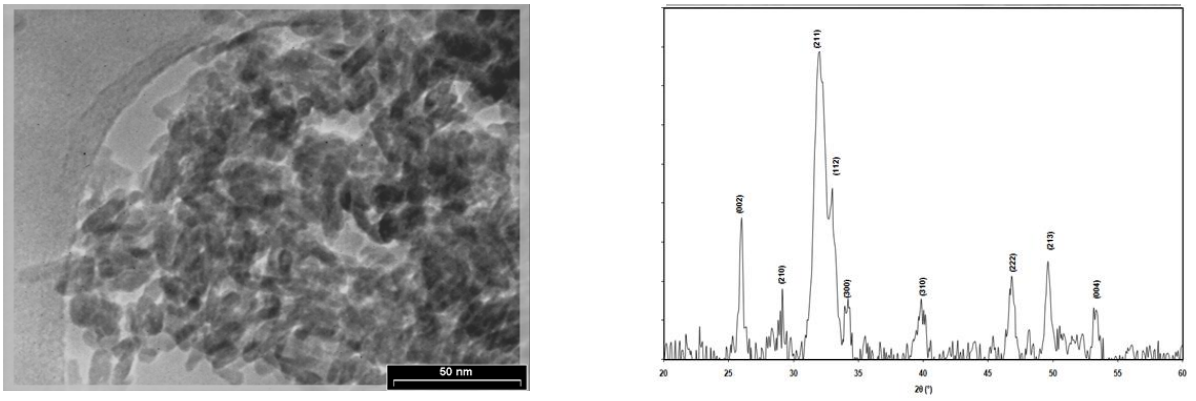


a) b)

**Fig. 1**. TEM micrograph (a) and XRD pattern (b) of nanocrystalline hydroxyapatite after drying at 373 K

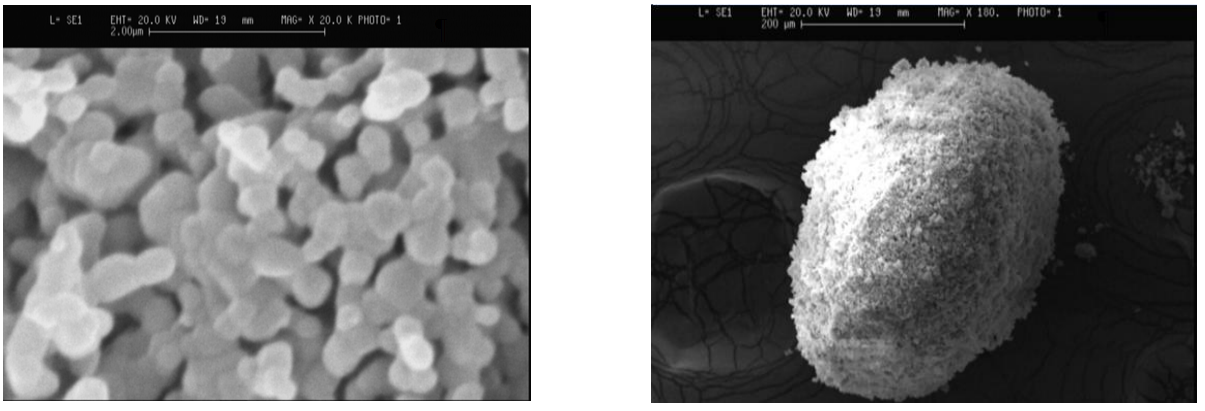


a) b)

**Fig. 2**. Morphology of granulated nano hydroxyapatite powders after granulation (a), and higher magnification of a granule (b)

### 3.2.2. Effect of lead initial concentration

The adsorption breakthrough curves obtained by changing lead initial concentration from 200 to 500 mg Pb/l at 10 ml/min flow rate and 10 mm bed depth are given in Fig. 4. As expected, a decrease in lead concentration gave a later breakthrough curve; the treated volume was the greatest at the lowest transport due to a decreased diffusion coefficient or mass transfer coefficient [27]. Exhaustion time occurred after 53 min at 200 mg/l lead initial concentration while the exhaustion time was 30 min at 500 mg/l. The exhaustion time decreased with increasing lead concentration as the binding sites became more quickly saturated in the column.

### 3.2.3. Effect of bed height

The accumulation of lead in a fixed-bed column is dependent on the quantity of adsorbent inside the column. In order to study the effect of bed height on lead retention, hydroxyapatite granules of three different bed heights, viz. 10, 15, and 20 mm, were used. A lead solution of fixed concentration (500 mg Pb/l) was passed through the fixed-bed column at a constant flow rate of 10 ml/min. As depicted by Fig. 5 the breakthrough curves varied with bed height. Steeper breakthrough curves were achieved with a decrease in bed depth. The exhaustion time decreased from 58 to 28 min with a decreasing bed depth from 20 to 10 mm, as binding sites were restricted at low bed depths. At low bed depth, the lead ions do not have enough time to diffuse into the surface of the hydroxyapatite granules, and a reduction in exhaustion time occurs. Conversely, with an increase in bed depth, the residence time of lead solution inside the column was increased, allowing the lead ions to diffuse deeper into the hydroxyapatite granules.

### 3.2.4. Adsorption modeling for breakthrough curve

#### 3.2.4.1. Thomas model

Successful design of a column lead adsorption process requires a description of the dynamic behavior of lead ion in a fixed bed. Various simple mathematical models

have been developed to describe and possibly predict the dynamic behavior of the bed in column performance [28]. One model used for continuous flow conditions is the Thomas model [29], which can be written as:

$$\ln\left(\frac{C_0}{C_e}-1\right)=\frac{k_{th}q_0m}{Q}-k_{th}C_0t \quad (1)$$

where, $k_{th}$ is the Thomas model constant, l/mg h; $q_0$ is the adsorption capacity, mg/g; $Q$ is the volumetric flow rate through the column, l/h; $m$ is the mass of adsorbent in the column, g; $C_0$ is the lead initial concentration, mg/l and $C_e$ is the lead effluent concentration, mg/l at any time $t$, h.

The Thomas model constants $k_{th}$ and $q_0$ were determined from a plot of $\ln[C_0/C_e-1]$ *vs.* $t$ at a given flow rate. The model parameters are given in Table 1. The Thomas model gave a good fit of the experimental data, at all the flow rates examined, with correlation coefficients greater than 0.965, which would indicate that the external and internal diffusions were not the rate limiting step [28]. The rate constant $k_{th}$ decreased with increasing lead initial concentration which indicates that the mass transport resistance increases. The reason is that the driving force for adsorption is the lead concentration difference between hydroxyapatite granules and solution [28, 30].

The breakthrough service time (BDST) model is based on physically measuring the capacity of the bed at various percentage breakthrough values. The BDST model constants can be helpful to scale up the process for other flow rates and concentrations without further experimentation. It is used to predict the column performance for any bed length, if data for some depths are known. It states that the bed depth, $Z$, and service time, $t$, of a column bears a linear relationship. The rate of adsorption is controlled by the surface reaction between adsorbate and the unused capacity of the adsorbent.

The BDST equation can be expressed as follows [29, 30]:

$$t=\frac{NZ}{C_0v}-\frac{1}{K_aC_0}\ln\left[\left(\frac{C_0}{C_b}\right)-1\right] \quad (2)$$

where $C_b$ is the lead breakthrough concentration, mg/l; $N$ is the adsorption capacity of bed, mg/l; $Z$ is the depth of column bed, cm; $v$ is the linear flow velocity of lead solution through the bed, ml/cm$^2$·h; $K_\alpha$ is the rate constant, l/mg·h.

### 3.2.4.2. Breakthrough service time (BDST) model

The column service time was selected as the time when the normalized concentration, $C_e/C_0$ reached 0.95. A plot of service time versus bed depth, at a flow rate of 10 ml/min (Fig. 6) was linear. The correlation coefficient value ($R^2$ = 0.986) indicated the validity of the BDST model for the present system. The values of BDST model parameters are presented in Table 1. The value of $K_\alpha$ characterizes the rate of transfer from the fluid phase to the solid phase. If $K_\alpha$ is large, even a short bed will avoid breakthrough, but as $K_\alpha$ decreases a progressively deeper bed is required to avoid breakthrough.

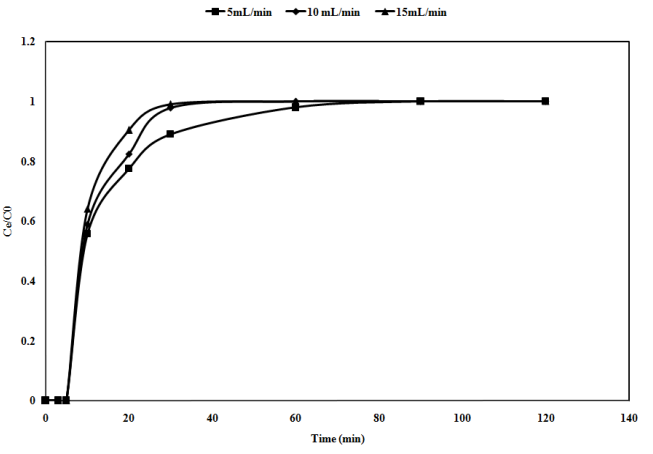


**Fig. 3.** Breakthrough curves expressed as $C_e/C_0$ *vs.* time at different flow rates (lead initial concentration 500 mg/l, initial pH 7.5, bed depth 10 mm and temperature 298±1 K)

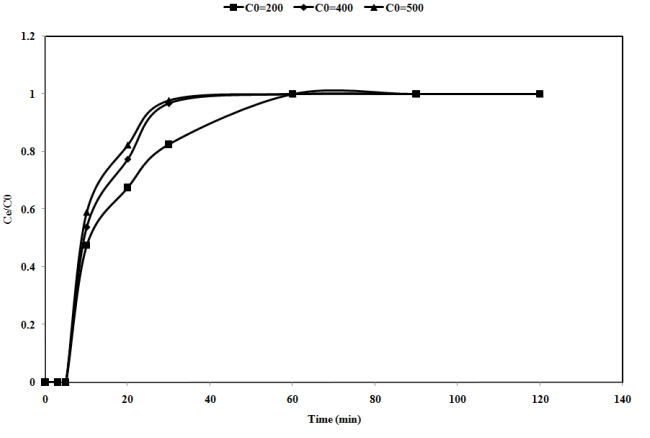


**Fig. 4.** Breakthrough curves expressed as $C_e/C_0$ *vs.* time at different lead concentrations (initial pH 7.5, flow rate 10 ml/min, bed depth 10 mm and temperature 298±1 K)

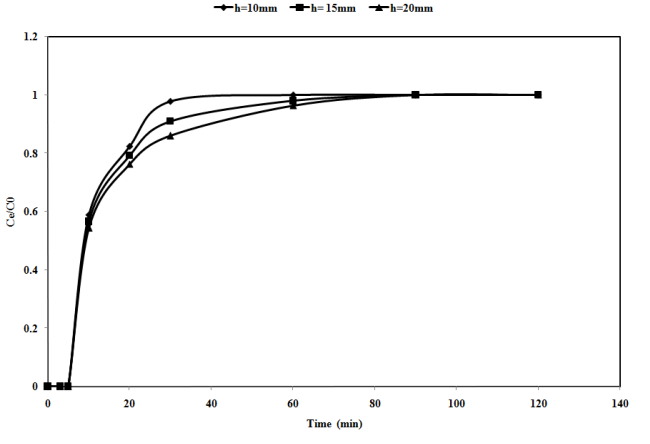


**Fig. 5.** Breakthrough curves expressed as $C_e/C_0$ *vs.* time at different bed depth (lead initial concentration 500 mg/l, initial pH 7.5, flow rate 10 ml/min and temperature 298±1 K)

*Table 1*

**The Thomas model and BDST model parameters for the adsorption of lead on nano hydroxyapatite granules**

| The Thomas model parameters | | | |
|---|---|---|---|
| Lead concentration, mg/l | $q_0$, mg/g | $k_{th}$, l/mg·h | $R^2$ |
| 200 | 993 | 0.00041 | 1 |
| 400 | 1796 | 0.00040 | 0.965 |
| 500 | 1972 | 0.00034 | 0.968 |
| The BDST model parameters | | | |
| $N$, mg/l | $K_a$, l/mg·h | | $R^2$ |
| 2500 | 0.072 | | 0.986 |

## 3.3. Absorbent Analysis after Absorption

Generally, HAp selectivity towards divalent metal cations is a result of the ion-exchange process with $Ca^{2+}$ ions [31]. Ionic radius of lead (1.19 Å) slightly differs from that of $Ca^{2+}$ (0.99 Å), and it can substitute $Ca^{2+}$ in the HAp crystal lattice. Fig. 7 presents the XRD patterns of $Pb^{2+}$-loaded sample after interaction of 10 mm bed depth of nano hydroxyapatite granules with 500 mg/l $Pb^{2+}$ solution, at flow rate of 10 ml/min. No structural changes of nano hydroxyapatite granules were detected by the powder X-ray diffraction analysis.

The sample was indexed in the hexagonal system with calcium lead hydroxide phosphate and hydroxypyromorphite ICSD name (Ref.Code.01-084-0814 and 00-008-0259 in XPERT software). The unit cell parameters of the starting nano Ca-HAp (Fig. 1b) were $a = b = 0.9424$ nm and $c = 0.6879$ nm, while values of $a = b = 0.9880$ nm and $c = 0.7417$ nm were calculated for the Pb-exchanged sample. These shifts are indicative to the increase in unit cell dimensions which is due to the replacement of $Ca^{2+}$ by $Pb^{2+}$ (ionic radius 1.19 Å), which is larger than $Ca^{2+}$ (ionic radius 0.99 Å), into the crystal lattice of apatite. These data strongly support the ion-exchange mechanism for $Pb^{2+}$ sorption by nano hydroxyapatite granules. The reaction mechanism corresponds to equimolar exchange of lead and calcium yielding $Ca_{10-x}Pb_x(PO_4)_6(OH)_2$, where $x$ can vary from 0 to 10 depending on the reaction time and experimental conditions. The proposed mechanism for lead removal by nano hydroxyapatite granules bed contains partial dissolution of calcium followed by the precipitation of an apatite by ion-exchange mechanism with the formula $Ca_{10-x}Pb_x(PO_4)_6(OH)_2$ [32], in which lead ions are first adsorbed on the nano hydroxyapatite granules surface and substitution with Ca occurs as described by the following equation:

$$Ca_{10}(PO_4)_6(OH)_2 + xPb^{2+} \rightarrow$$
$$\rightarrow Ca_{10-x}Pb_x(PO_4)_6(OH)_2 + xCa^{2+}$$

In case of complete replacement of calcium by lead, hydroxypyromorphite phase with $Pb_{10}(PO_4)_6(OH)_2$ formula is formed.

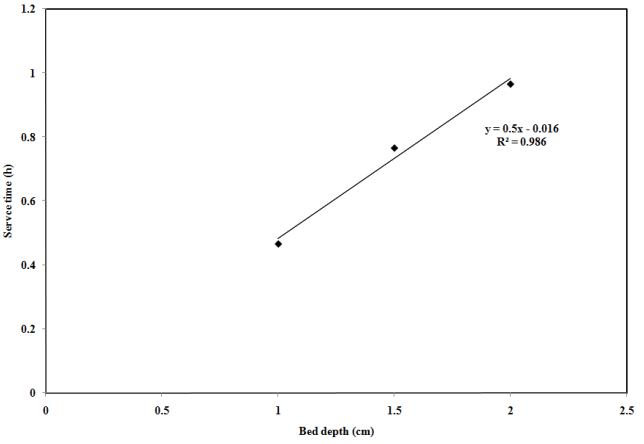


**Fig. 6.** Plot of BDST equation for lead adsorption on nano hydroxyapatite granules

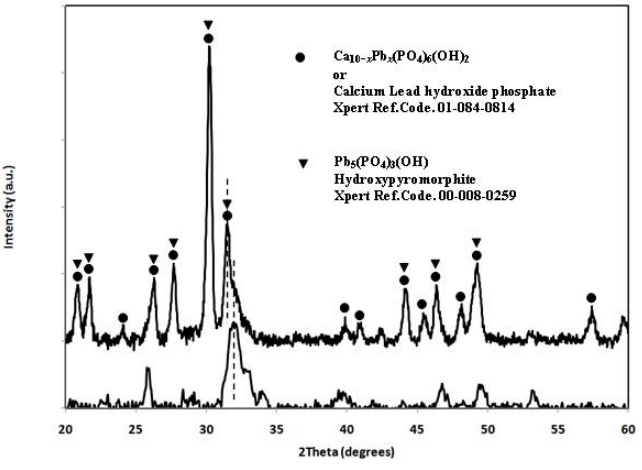


**Fig. 7.** XRD patterns of $Pb^{2+}$-loaded nano hydroxyapatite granules sample after adsorption

The TEM of $Pb^{2+}$-loaded nano hydroxyapatite granules sample is shown in Fig. 8a. The microstructure of HAp after adsorption was almost of needle shape, with a size in the range of 20–30 nm and rod shape particle with a square cross-sectional with the length of about 200 to 500 nm. Fig. 8b shows the EDS analysis of A and B points

of Fig. 8a, that indicated needle shape, with a size in the range of 20–30 nm "A" contains Ca, Pb, P, Cu and O, the rod shape particle with a square cross-sectional "B" contain Pb, P, Cu and O elements. Thus, according to TEM micrographs, and EDS patterns, it is demonstrated that the needle shape particle in the range of 20–30 nm "A" is $Ca_{10-x}Pb_x(PO_4)_6(OH)_2$, and rod shape particle with a square cross-sectional "B" were $Pb_{10}(PO_4)_6(OH)_2$. In addition, Cu peaks were also observed in the EDS spectrum. The peaks for Cu arise from stray scattering of X-rays from the copper grid.

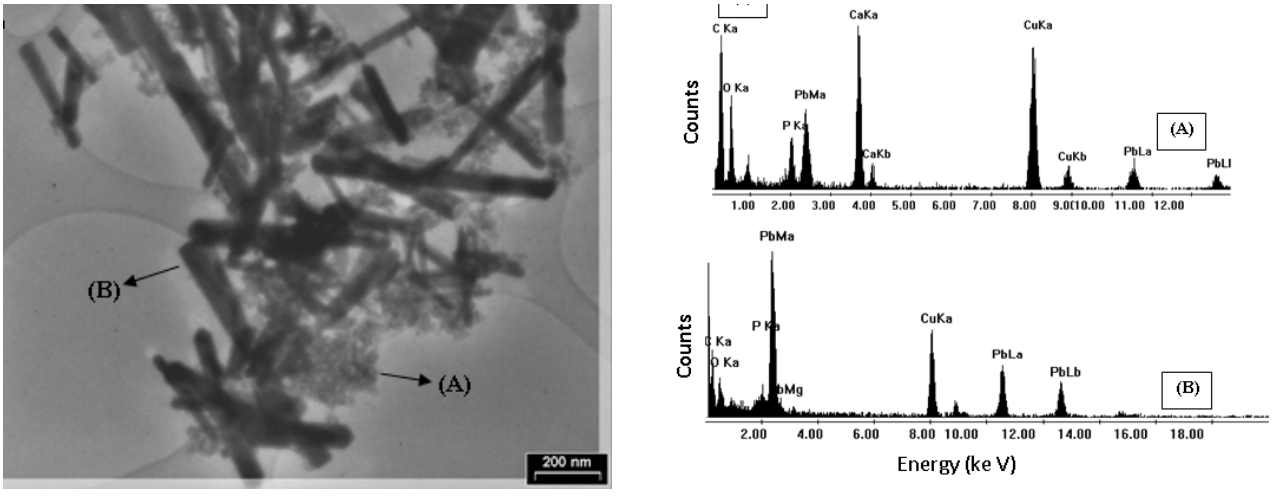


a) b)

**Fig. 8.** TEM micrograph (a) and EDS spectrum of $Pb^{2+}$-loaded the nano hydroxyapatite granules sample after adsorption (b)

## 4. Conclusions

Thomas and BDST models were successfully used for predicting breakthrough curves for lead removal by a fixed bed of nano hydroxyapatite granules using different initial lead concentration and bed depths with correlation coefficients greater than 0.965. The breakthrough time and exhaustion time decreased with increasing flow rate, decreasing bed depth and increasing influent lead concentration. The results of XRD and TEM analysis strongly supported the ion exchange as a main mechanism for $Pb^{2+}$ cations removal by nano hydroxyapatite granules fixed bed. The results showed that the lead uptake by nano hydroxyapatite proceeded with a rapid surface complexation of lead on the surface site prior to the formation of compounds with the formula $Ca_{10-x}Pb_x(PO_4)_6(OH)_2$ and $Pb_{10}(PO_4)_6(OH)_2$. Therefore, the use of nano hydroxyapatite granules as an adsorbent for lead removal is potentially effective and may provide an alternative method for lead removal from contaminated water.

## References

[1] Huang X., Sillanpëë M., Dou B., Gjessing E.T.: Environ. Pollut., 2008, **156**, 270. https://doi.org/10.1016/j.envpol.2008.02.014
[2] Aman T., Kazi A., Sabri M., Bano Q.: Colloid Surface B, 2008, **63**, 116. https://doi.org/10.1016/j.colsurfb.2007.11.013
[3] Jiang Y., Pang H., Liao B.: J. Hazard. Mater., 2009, **164**, 1. https://doi.org/10.1016/j.jhazmat.2008.07.107
[4] Brostow W., Hagg Lobland H.: Materials: Introduction and Applications, John Wiley & Sons, New York 2017.
[5] ISIRI, (Bureau of Iran Standards) 1053, fifth revision, 2009.
[6] FAO/WHO, Evaluation of certain food additives and contaminants WHO, Lead in drinking-water 2011.
[7] Squadrone S., Prearo M., Brizio P. *et al.*: Chemosphere, 2013, **90**, 358. https://doi.org/10.1016/j.chemosphere.2012.07.028
[8] Martin-Lara M., Blázquez G., Ronda A. *et al.*: J. Ind. Eng. Chem., 2012, **18**, 1006. https://doi.org/10.1016/j.jiec.2011.11.150
[9] Kalkan E., Akbulut S.: Eng. Geolog., 2004, **73**, 145. https://doi.org/10.1016/j.enggeo.2004.01.001
[10] Kalkan E.: Appl. Clay Sci., 2009, **43**, 296. https://doi.org/10.1016/j.clay.2008.09.002
[11] Zheng W., Li X., Wang F. *et al.*: J. Hazard. Mater., 2008, **157**, 490. https://doi.org/10.1016/j.jhazmat.2008.01.029
[12] Krestou A., Xenidis A., Panias D.: Miner. Eng., 2004, **17**, 373. https://doi.org/10.1016/j.mineng.2003.11.019
[13] Chen X., Wright J., Conca J., Peurrung L.: Environ. Sci. Technol., 1997, **31**, 624. https://doi.org/10.1021/es950882f
[14] Czerniczyniec M., Farias S., Magallanes J., Cicerone D.: 11th Int. Conf. on Surface and Colloid Science, Brazil 2003, 269.
[15] Vega E., Pedregosa J., Narda G.: J. Phys. Chem. Solids, 1999, **60**, 759. https://doi.org/10.1016/s0022-3697(98)00340-0
[16] Reichert J., Binner J.: J. Mater Sci., 1996, **31**, 1231. https://doi.org/10.1007/bf00353102
[17] Leyva A., Marrero J., Smichowski P., Cicerone D.: Environ. Sci. Technol., 2001, **35**, 3669. https://doi.org/10.1021/es0009929
[18] Fuller C., Bargar J., Davis J., Piana M.: Environ. Sci. Technol., 2002, **36**, 158. https://doi.org/10.1021/es0108483
[19] McGrellis S., Serafini J., Jean J. *et al.*: Sep. Purif. Technol., 2001, **24**, 129. https://doi.org/10.1016/s1383-5866(00)00223-9

[20] Zamani S., Salahi E., Mobasherpour I.: Res. Chem. Intermed., 2014, **40**, 1753. https://doi.org/10.1007/s11164-013-1078-3
[21] Mobasherpour I., Salahi E., Pazouki M.: J. Saudi Chem. Soc., 2011, **15**, 105. https://doi.org/10.1016/j.jscs.2010.06.003
[22] Baral S., Das N., Ramulu T. *et al.*: J. Hazard. Mater., 2009, **161**, 1427. https://doi.org/10.1016/j.jhazmat.2008.04.127
[23] Calero M., Hernáinz F., Blázquez G. *et al.*: J. Hazard. Mater., 2009, **171**, 886. https://doi.org/10.1016/j.jhazmat.2009.06.082
[24] Mobasherpour I., Soulati Heshajin M., Kazemzadeh A., Zakeri M.: J. Alloy Compd., 2007, **430**, 330. https://doi.org/10.1016/j.jallcom.2006.05.018
[25] Bhakat P., Gupta A., Ayoob S.: J. Hazard. Mater., 2007, **139**, 286. https://doi.org/10.1016/j.jhazmat.2006.06.037
[26] Ozdemir O., Turan M., Turan A. *et al.*: J. Hazard. Mater., 2009, **166**, 647. https://doi.org/10.1016/j.jhazmat.2008.11.123
[27] Uddin M., Rukanuzzaman M., Rahman Khan M., Islam M.: J. Environ. Manage., 2009, **90**, 3443. https://doi.org/10.1016/j.jenvman.2009.05.030
[28] Aksu Z., Gonen F.: Process. Biochem., 2004, **39**, 599. https://doi.org/10.1016/s0032-9592(03)00132-8
[29] Thomas H.: J. Am. Chem. Soc., 1944, **66**, 1664. https://doi.org/10.1021/ja01238a017
[30] Han R., Zhang J., Zou W. *et al.*: J. Hazard. Mater., 2006, **133**, 262. https://doi.org/10.1016/j.jhazmat.2005.10.019
[31] Monteil Rivera F., Fedoroff M.: Encyclopedia of Surface and Colloid Science. Marcel Dekker. Inc, New York 2002.
[32] Baillez S., Nzihou A., Bernache-Assolant D. *et al.*: J. Hazard. Mater., 2007, **A139**, 443. https://doi.org/10.1016/j.jhazmat.2006.02.039

*Received: July 05, 2017 / Revised: November 07, 2017 / Accepted: January 09, 2018*

## АДСОРБЦІЯ СВИНЦЮ НАНОГРАНУЛАМИ ГІДРОКСИАПАТИТУ В КОЛОНІ З НЕРУХОМИМ ШАРОМ

***Анотація***. *З використанням гідроксиапатитових наногранул проведено сорбцію йонів $Pb^{2+}$ в колоні з нерухомим шаром. Визначено, що час проникнення до розривання та вичерпування зменшувався зі збільшенням швидкості потоку, зменшенням глибини шару та збільшенням початкової концентрації свинцю. Запропоновано механізм процесу – часткове розчинення кальцію з наступним висадженням апатиту згідно йонообмінного механізму з формулою $Ca_{10-x}Pb_x(PO_4)_6(OH)_2$ і $Pb_{10}(PO_4)_6(OH)_2$.*

*Ключові слова: наногранули гідроксиапатиту, $Pb^{2+}$, адсорбція, видалення, нерухомий шар.*